

19. BASALTS FROM THE ATLANTIC CRUST WEST OF THE BARBADOS RIDGE (SITE 543, LEG 78A): GEOCHEMISTRY AND MINERALOGY¹

H. Bougault, J. L. Joron, R. C. Maury, M. Bohn, M. Tardy, and B. Biju-Duval²

ABSTRACT

The upper part of the basaltic substratum of the Atlantic abyssal plain, approaching subduction beneath the Barbados Ridge and thus presumably beneath the Lesser Antilles island arc, is made of typical LREE-depleted oceanic tholeiites. Mineralogical (microprobe) and geochemical (X-ray fluorescence, neutron activation analyses) data are given for 12 samples from the bottom of Hole 543A, which is 3.5 km seaward of the deformation front of the Barbados Ridge complex. These basalts are overlain by a Quaternary to Maestrichtian–Campanian sedimentary sequence. Most of the basalts are relatively fresh (in spite of the alteration of olivine and development of some celadonite, clays, and chlorite in their groundmass), and their mineralogical and geochemical compositions are similar to those of LREE-depleted recent basalts from the Mid-Atlantic Ridge. The most altered samples occur at the top of the basaltic sequence, and show trends of enrichment in alkali metals typical of altered oceanic tholeiites.

INTRODUCTION

Site 543 was located on the Atlantic abyssal plain, 3.5 km seaward of the deformation front of the Barbados Ridge complex (Fig. 1). The basaltic substratum, overlain by a Quaternary to Maestrichtian–Campanian sedimentary sequence, was reached at 411 m sub-bottom and drilled down to 455 m sub-bottom in Hole 543A. Recovered were 35.9 m of basalt, among which 12 samples (listed in Table 1) were made available to us (Fig. 2). The basalts appeared to be exclusively constituted by pillows, and 59 separate cooling units (presumably corresponding to individual pillows) were identified (see Site 543 report, this volume). The 12 samples studied respectively belong to Cooling Units 3, 8, 10, 18, 23, 28, 32, 36, 46, 51, 53, and 58. Geochemical (major and trace elements) and mineralogical (microprobe) investigations were conducted on these 12 samples, with two major goals: (1) characterization of the oceanic crust subducting beneath the Barbados Ridge and thus presumably beneath the Lesser Antilles island arc; and (2) comparison with Mid-Atlantic Ridge basalts.

LITHOLOGY

The samples are relatively fresh, though all of them have been altered, with various degrees of development of celadonite, clays, and chlorite in the groundmass, alteration of olivine to chlorite or serpentine, oxidation of titanomagnetite, and filling of void spaces by calcite. Alteration is more important at the top of the basaltic sequence, where secondary orthoclase (adularia-type) has been found.

Phenocrysts are invariably present, though in low amounts (usually less than 10%): they include olivine, invariably altered but containing fresh spinel inclusions; plagioclase, often reaching several millimeters in size; clinopyroxene, apparently lacking at the top of the sequence but occurring sporadically in samples from Cores 13 through 16.

The composition of the groundmass depends upon the position of the sample in the cooling unit: all the transitions are observed between glassy margins of pillows and well-crystallized microlitic cores (plagioclase + clinopyroxene + titanomagnetite + secondary minerals).

MAJOR ELEMENT COMPOSITIONS

The 12 analyses presented in Table 1 are typical of oceanic tholeiites. The compositions are fairly constant, the most striking variations reflecting the pattern of alteration: the top samples (543A-10-3, 27–31 cm, 543A-11-2, 34–36 cm, and 543A-12-2, 56–59 cm) are enriched in K₂O and somewhat depleted in SiO₂ with respect to others; these variations are correlated with higher values of the loss on ignition.

It is thus difficult to distinguish chemical units in the basaltic sequence; nevertheless, the three bottom samples (543A-16-3, 117–120 cm, 543A-16-5, 32–35 cm, and 543A-16-7, 60–63 cm) appear to be slightly SiO₂-enriched, and MgO- and MnO-depleted with respect to the others.

MINERALOGY (PRIMARY MINERALS)

Spinel (Table 2) are found either as inclusions in altered olivine phenocrysts or as individual crystals (up to 200 μ m in size). Their compositions are fairly constant, fall in the range of magnesiochromites with $Mg/(Mg + Fe^{2+}) = 0.60\text{--}0.64$ and $Cr/(Cr + Al) = 0.49\text{--}0.52$, and are similar to the most abundant spinel type found in Mid-Atlantic Ridge basalts (Sigurdsson and Schilling, 1976). The samples in which they have been found are not enriched in Cr with respect to the other bulk rocks.

¹ Biju-Duval, B., Moore, J. C., et al., *Init. Repts. DSDP, 78A*: Washington (U.S. Govt. Printing Office).

² Addresses: (Bougault, Bohn) Centre Océanologique de Bretagne, CNEXO, B.P. 337, 29273 Brest, France and G.I.S. 410012; (Joron) Laboratoire P. Sûe, CNRS, CEN Saclay, B.P. 2, 91190 Gif-sur-Yvette, France; (Maury) (Bohn) Laboratoire de Pétrologie, Université de Bretagne Occidentale, 29283 Brest, France and G.I.S. 410012; (Tardy) Département des Sciences de la Terre, Université de Savoie, B.P. 143, 73011 Chambéry, France; (Biju-Duval, present address: Centre National pour l'Exploitation des Océans, 66 Avenue d'Iéna, 75116 Paris, France).

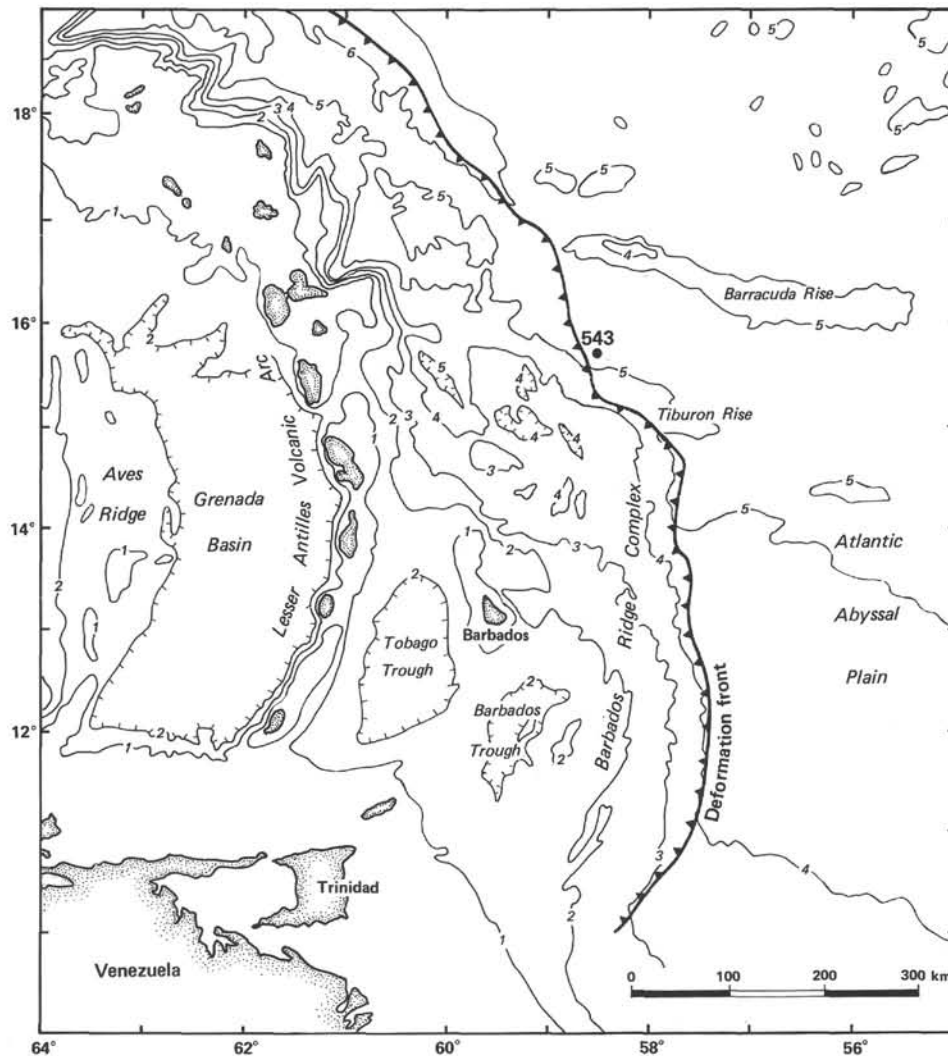


Figure 1. Location of Site 543, east of the deformation front of the Barbados Ridge. Contours in kilometers.

Clinopyroxenes (Table 3). The phenocrysts, when present, are iron-poor ($\text{FeO} = 4.6\%$; Analyses 8–10) and plot near the endiopside-augite boundary of the Ca-Mg-(Fe + Mn) diagram (Fig. 3). They differ consistently from the groundmass pyroxenes and microphenocrysts by their lower TiO_2 and Al_2O_3 contents and higher MgO and Cr_2O_3 (up to 0.9%) amounts. The large crystals up to several millimeters in length (Analyses 8, 9, 10, Table 3), found in Sample 543A-13-2, 133–136 cm, are similar in composition to some phenocrysts found in North Atlantic basalts (Wood et al., 1979); considering their high $\text{Mg}/(\text{Mg} + \text{Fe})$ ratios (0.88–0.85) and temperatures of equilibration with their bulk host rock (1190–1170°C following the method of Nielsen and Drake, 1979), they may well represent early-crystallized phenocrysts.

The groundmass and microphenocryst clinopyroxenes show a considerable scatter of compositional variations in the Ca-Mg-(Fe + Mn) diagram (Fig. 3): some of them plot in the ferroaugite (Analysis 25), subcalcic augite (15, 21), or salite (12, 13, 26) fields. In fact, the most iron-rich compositions are those of very small and presumably late-crystallized pyroxenes in the groundmass

of pillow cores. Figure 3B shows that the compositional scatter of pyroxenes from individual samples is more restricted than that in the composite. The trends of the pyroxenes from predominantly glassy samples from pillow margins (e.g., 543A-16-7, 60–63 cm) do not show iron enrichment, and may be considered as quench trends (Smith and Lindsley, 1971); on the contrary, the trends of pyroxenes from relatively slowly-cooled pillow cores are more or less parallel to the Mg-(Fe + Mn) side of the diagram, and show the iron enrichment typical of tholeiitic pyroxenes.

Plagioclases (Table 4). Their whole compositional range is An_{88} to An_{37} ; roughly, the cores of phenocrysts vary from An_{88} to An_{65} , and most of the groundmass crystals from An_{65} to An_{55} or sometime less. Their orthoclase content is generally lower than 0.5%, and they usually contain appreciable amounts of MgO, as do most ocean-floor plagioclases (Hawkins, 1977).

Figure 4 shows some zoning patterns of plagioclases of various sizes: large and often rounded crystals, and smaller ones. There is no definite relation between the size of plagioclases and their compositions; the cores of

Table 1. Basalts from Hole 543A: major element analyses (wt.%) and CIPW norms.

| | Sample (interval in cm) | | | | | | | | | | | | |
|----------------------------------|----------------------------|---------------------|---------------------|----------------------|-----------------------|---------------------|---------------------|---------------------|---------------------|-----------------------|---------------------|---------------------|-------|
| | 543A-10-3, 27-31 | 543A-11-2, 34-36 | 543A-12-2, 56-59 | 543A-12-4, 99-101 | 543A-13-2, 133-136 | 543A-13-5, 84-87 | 543A-14-1, 33-36 | 543A-15-3, 71-74 | 543A-16-2, 34-37 | 543A-16-3, 117-120 | 543A-16-5, 32-35 | 543A-16-7, 60-63 | |
| SiO ₂ | 49.65 | 49.43 | 49.92 | 50.63 | 50.82 | 50.95 | 50.85 | 50.62 | 50.29 | 50.84 | 50.58 | 51.24 | |
| TiO ₂ | 1.74 | 1.70 | 1.98 | 1.60 | 1.55 | 1.55 | 1.49 | 1.51 | 1.62 | 1.52 | 1.65 | 1.50 | |
| Al ₂ O ₃ | 17.08 | 16.12 | 15.05 | 16.15 | 15.92 | 15.89 | 15.93 | 15.50 | 15.68 | 16.36 | 16.17 | 15.89 | |
| Fe ₂ O ₃ * | 10.95 | 10.71 | 11.62 | 10.06 | 10.15 | 9.85 | 9.84 | 9.94 | 10.45 | 9.34 | 10.42 | 10.16 | |
| MnO | 0.21 | 0.19 | 0.22 | 0.17 | 0.18 | 0.18 | 0.19 | 0.19 | 0.20 | 0.16 | 0.18 | 0.17 | |
| MgO | 6.63 | 6.80 | 7.01 | 6.47 | 6.72 | 7.01 | 7.48 | 7.80 | 7.01 | 6.18 | 6.61 | 6.56 | |
| CaO | 8.95 | 11.53 | 10.74 | 12.10 | 12.33 | 10.12 | 12.27 | 12.21 | 12.22 | 12.99 | 12.35 | 12.42 | |
| Na ₂ O | 2.80 | 2.80 | 2.90 | 2.75 | 2.60 | 2.40 | 2.50 | 2.55 | 2.65 | 2.45 | 2.70 | 2.60 | |
| K ₂ O | 1.88 | 0.36 | 0.75 | 0.27 | 0.16 | 0.19 | 0.02 | 0.02 | 0.06 | 0.42 | 0.11 | 0.22 | |
| P ₂ O ₅ | 0.23 | 0.21 | 0.21 | 0.21 | 0.20 | 0.21 | 0.21 | 0.19 | 0.23 | 0.16 | 0.21 | 0.18 | |
| Total | 100.12 | 99.85 | 100.40 | 100.41 | 100.63 | 98.35 | 100.78 | 100.53 | 100.41 | 100.42 | 100.98 | 100.94 | |
| Loss on ignition 1050° | 3.68 | 2.09 | 1.34 | 1.20 | 1.32 | 1.01 | 0.94 | 0.77 | 1.42 | 1.52 | 1.49 | 1.32 | |
| Q | | | | | 0.47 | 3.70 | 0.49 | | | 0.64 | | 0.80 | |
| or | | | | | 0.95 | 1.15 | 0.12 | 0.36 | | 2.49 | 0.65 | 1.30 | |
| ab | 23.86 | 23.93 | 24.66 | 23.35 | 22.03 | 20.81 | 21.15 | 21.63 | 22.51 | 20.79 | 22.81 | 21.97 | |
| an | 28.71 | 30.67 | 25.98 | 31.05 | 31.36 | 32.83 | 32.19 | 30.88 | 30.85 | 32.51 | 31.64 | 31.01 | |
| di | wo | 6.12 | 10.80 | 11.00 | 11.68 | 12.00 | 7.29 | 11.46 | 12.00 | 11.97 | 13.02 | 11.82 | 12.31 |
| | en | 3.45 | 6.20 | 6.24 | 6.73 | 6.96 | 4.31 | 6.93 | 7.33 | 6.98 | 7.59 | 6.78 | 7.06 |
| | fs | 2.42 | 4.12 | 4.30 | 4.41 | 4.48 | 2.57 | 3.91 | 3.99 | 4.43 | 4.82 | 4.51 | 4.69 |
| en | 3.51 | 6.16 | 5.71 | 8.97 | 9.80 | 13.58 | 11.69 | 11.67 | 9.97 | 7.85 | 9.27 | 9.25 | |
| fs | 2.46 | 4.10 | 3.94 | 5.89 | 6.31 | 8.09 | 6.59 | 6.36 | 6.33 | 4.98 | 6.17 | 6.15 | |
| fo | 6.78 | 3.32 | 3.93 | 0.33 | | | | 0.34 | 0.40 | | 0.27 | | |
| fa | 5.23 | 2.43 | 2.98 | 0.24 | | | | 0.20 | 0.28 | | 0.20 | | |
| mt | 2.40 | 2.36 | 2.54 | 2.20 | 2.21 | 2.20 | 2.15 | 2.17 | 2.29 | 2.04 | 2.26 | 2.20 | |
| il | 3.33 | 3.26 | 3.78 | 3.05 | 2.95 | 3.02 | 2.83 | 2.88 | 3.09 | 2.90 | 3.13 | 2.85 | |
| ap | 0.55 | 0.50 | 0.50 | 0.50 | 0.48 | 0.51 | 0.50 | 0.45 | 0.55 | 0.38 | 0.50 | 0.43 | |
| S.I. | 31.32 | 34.70 | 33.20 | 34.88 | 36.11 | 37.95 | 39.66 | 40.39 | 36.66 | 35.40 | 35.17 | 35.42 | |
| D.I. | 35.06 | 26.07 | 29.12 | 24.95 | 23.45 | 25.65 | 21.76 | 21.75 | 22.87 | 23.92 | 23.45 | 24.06 | |

Note: Fe₂O₃* = total iron as Fe₂O₃. The CIPW norms are calculated with 85% of total iron as FeO and 15% as Fe₂O₃. S.I. = Solidification Index. D.I. = Differentiation Index.

the largest crystals are fairly homogeneous from the chemical point of view, and their more sodic rims approximate the composition of the groundmass micro-lites. The cores of the smallest crystals, presumably of latest appearance (Natland, 1979), show some indications of predominantly reverse zoning, however, their overall compositional range is the same as that of larger plagioclases.

TRACE ELEMENT COMPOSITIONS

The trace element compositions of basalts sampled in Hole 543A are given in Table 5; the elements are presented in the order of increasing atomic number, including Ti, Mn, and Fe (all concentrations are expressed in ppm). All measurements were made either by X-ray fluorescence spectrometry (XRF) at COB (Centre Océanologique de Bretagne) (Bougault et al., 1977; Bougault, 1980) or by instrumental neutron activation (NAA) at P. Süe Laboratory (Treuil et al., 1973). The analytical method is indicated in Table 5 for each element.

A first look at Table 5 shows that the concentrations of trace elements of these samples are typical of oceanic tholeiites. Nevertheless, some variations are observed within these samples; it is necessary to show in precisely what way some concentrations of elements are characteristic of ocean tholeiites and to what extent some variations are the result of secondary processes. We will consider successively alkali elements, elements with high mineral-liquid partition coefficients (Ni and Cr), and hygromagmaphile elements.

The uptake of alkali elements during low temperature alteration is a well-known process. A good example was

found in Holes 417A and 418 drilled during Legs 51 and 52 (Donnelly et al., 1979). The variation of the concentrations of alkali elements (Rb, Cs in Table 5 and K₂O in Table 1) in basaltic samples of Hole 543A are well correlated with the loss on ignition and are without any doubt the result of alteration processes. This observation is in agreement with the comments dealing with the description of samples. Very probably the variations observed for the other elements (major and trace), even if in a narrower range than for alkali metals, are the consequence of this alteration. This implies that the 12 analyzed samples represent a single magmatic unit whose initial composition (before alteration) is given by the composition of Samples 543A-14-1, 33-36 cm and 543A-15-3, 71-74 cm. It is interesting to note that the concentrations of K₂O (0.2%), Rb (1 ppm) and Cs (<0.02 ppm) for these samples are very low; this is typically characteristic of ocean tholeiites. As a consequence, the amounts of alkali elements measured in other samples correspond almost completely to the uptake of the elements from seawater. Rubidium is plotted versus cesium in Figure 5; the ratio Rb/Cs, about 200, which again is the result of uptake from seawater and not an original feature of the rocks, is very similar to the value obtained from Hole 417A samples (Leg 51, Bougault et al., 1979). This similarity confirms that the alteration of the ocean crust plays an important role in the budget of alkali elements in seawater.

A significant difference in the behavior of the two high partition coefficient elements, Cr and Ni, can be observed. Cr concentration is almost constant within studied samples (233-284 ppm), whereas Ni varies from 65

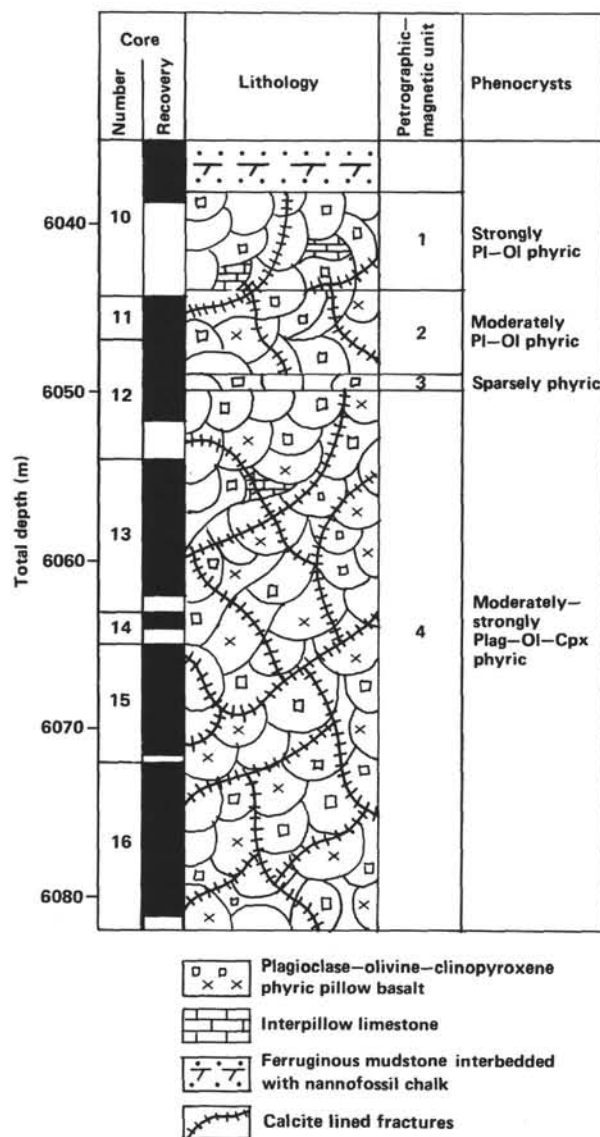


Figure 2. Summary lithology column of igneous rocks cored at Site 543, giving core numbers, recovery, petrographic-magnetic units (see Site 543 report; and Wilson, this volume), and summary petrography.

to 115 ppm (XRF data). We believe that this range of variation of Ni is not a primary feature (fractional crystallization of olivine) but the result of alteration processes. This statement is supported by correlation of Ni values with alkali element concentrations and losses on ignition. In addition, this correlation extends to MgO values; during magmatic processes Ni is principally concentrated in olivine, and because olivine is destroyed, Ni may be leached out together with Mg. On the contrary, Cr is concentrated in spinels and clinopyroxenes, which are well preserved compared to olivine minerals. We would thus conclude that the concentrations of Ni (115 ppm) and Cr (250 ppm) in the less altered samples are typical values of these oceanic tholeiites and that the lower values found for Ni reflect leaching processes in the most altered samples.

Table 2. Magnesiochromite analyses (wt.%) and their structural formulas.

| Sample (interval in cm) | 543A-13-2, 133-136 | | 543A-16-7, 60-63 | | |
|--------------------------------|-----------------------|-------|---------------------|--------|-------|
| | 1 | 2 | 3 | 4 | 5 |
| Analysis no. | | | | | |
| SiO ₂ | 0.04 | 0.07 | 0.10 | 0.08 | 0.02 |
| TiO ₂ | 0.63 | 0.57 | 0.43 | 0.53 | 0.48 |
| Al ₂ O ₃ | 24.69 | 24.84 | 27.16 | 25.97 | 26.26 |
| Cr ₂ O ₃ | 39.06 | 39.75 | 38.41 | 38.97 | 38.08 |
| Fe ₂ O ₃ | 6.08 | 5.38 | 4.80 | 6.16 | 5.63 |
| FeO | 15.06 | 15.60 | 14.49 | 14.40 | 14.12 |
| MnO | 0.20 | 0.19 | 0.03 | 0.25 | 0.19 |
| MgO | 13.73 | 13.43 | 14.42 | 14.47 | 14.36 |
| CaO | 0.00 | 0.10 | 0.08 | 0.15 | 0.10 |
| Total | 99.49 | 99.93 | 99.92 | 100.98 | 99.24 |
| Si | 0.009 | 0.017 | 0.023 | 0.020 | 0.005 |
| Ti | 0.116 | 0.104 | 0.077 | 0.095 | 0.087 |
| Al | 7.103 | 7.125 | 7.670 | 7.308 | 7.492 |
| Cr | 7.538 | 7.651 | 7.271 | 7.357 | 7.290 |
| Fe ³⁺ | 1.117 | 0.985 | 0.865 | 1.106 | 1.026 |
| Fe ²⁺ | 3.075 | 3.176 | 2.904 | 2.875 | 2.858 |
| Mn | 0.041 | 0.039 | 0.006 | 0.051 | 0.038 |
| Mg | 4.996 | 4.873 | 5.151 | 5.149 | 5.181 |
| Ca | 0.000 | 0.027 | 0.019 | 0.037 | 0.026 |

Note: Analysis nos. 1 and 2: core and rim of a crystal 150 μ m in size; Analysis nos. 3-5: inclusions into olivine phenocrysts. Fe³⁺ has been estimated by stoichiometry to 24 cations and 32 oxygens. All the microprobe analyses presented in this chapter (Tables 2-4) have been obtained with a Camebax-type automated microprobe (Microsonde Ouest, Brest; working conditions 15 Kv, 10 mA; counting time: 6s).

The range of variation of hygromagmaphile elements is shown in Figure 6 where these elements are plotted on an extended Coryell-Masuda diagram (Bougault, 1980). These patterns with low Th, Ta, and La values normalized to chondrite are typical of "depleted" oceanic tholeiites. In addition, the La/Ta ratio is equal to 18; this is also characteristic of depleted ocean tholeiites (Bougault et al., 1979). Except for Sample 543A-16-3, 117-120 cm, which corresponds to the upper pattern in Figure 6, the range of variation of the concentrations of hygromagmaphile elements within these samples is the consequence of alteration. These elements do not move with low temperature alteration; the consequence is that higher values are observed for altered samples.

DISCUSSION

Hole 543A Samples Compared to Mid-Atlantic Ridge Basalts

A considerable amount of geochemical and mineralogical data are now available on Mid-Atlantic Ridge basalts. From the petrological, mineralogical, and chemical (major elements) points of view, evidence from the data already discussed indicates that Site 543 basalts do not depart in any way from the usual characteristics of Mid-Atlantic Recent basalts. A striking point is that if we exclude the extensively altered rocks from the top of the basaltic sequence of Hole 543A (3 samples), the larger part of that sequence is made of relatively fresh basalts

Table 3. Clinopyroxene analyses (wt.%).

| Sample (interval in cm) | 543A-11-2, 34-36 | | | | 543A-13-2, 133-136 | | | | 543A-14-1, 33-36 | | | | 543A-15-3, 71-74 | | | | 543A-16-5, 32-35 | | 543A-16-7, 60-63 | | | | | |
|--------------------------------|---------------------|-------|-------|-------|-----------------------|-------|-------|-------|---------------------|--------|-------|--------|---------------------|-------|-------|-------|---------------------|-------|---------------------|--------|-------|-------|-------|-------|
| | 6 | 7 | 8 | 9 | 10 | 11 | 12 | 13 | 14 | 15 | 16 | 17 | 18 | 19 | 20 | 21 | 22 | 23 | 24 | 25 | 26 | 27 | 28 | 29 |
| SiO ₂ | 49.42 | 47.40 | 53.01 | 52.42 | 51.49 | 47.69 | 45.46 | 46.39 | 48.90 | 54.49 | 50.43 | 50.29 | 50.01 | 49.22 | 49.58 | 51.97 | 52.78 | 50.68 | 50.17 | 51.19 | 47.54 | 49.06 | 51.54 | 51.16 |
| TiO ₂ | 1.72 | 2.29 | 0.28 | 0.42 | 0.73 | 2.21 | 3.33 | 3.42 | 1.64 | 0.34 | 1.03 | 1.31 | 1.26 | 1.46 | 1.45 | 0.61 | 0.69 | 1.03 | 1.32 | 0.79 | 2.50 | 1.71 | 0.63 | 0.94 |
| Al ₂ O ₃ | 6.46 | 5.14 | 2.27 | 2.74 | 3.98 | 5.70 | 7.31 | 5.51 | 3.16 | 1.69 | 5.14 | 4.29 | 3.01 | 3.02 | 2.60 | 0.93 | 2.69 | 3.61 | 3.50 | 1.29 | 6.01 | 4.57 | 3.73 | 3.75 |
| Cr ₂ O ₃ | 0.09 | 0.26 | 0.69 | 0.89 | 0.24 | 0.23 | 0.09 | 0.41 | 0.09 | 0.44 | 0.61 | 0.22 | 0.00 | 0.00 | 0.00 | 0.00 | 0.25 | 0.00 | 0.00 | 0.04 | 0.15 | 0.33 | 0.59 | 0.61 |
| FeO | 8.23 | 11.36 | 4.36 | 4.99 | 6.01 | 9.73 | 9.33 | 9.76 | 15.10 | 7.52 | 5.97 | 8.54 | 10.70 | 15.77 | 17.31 | 19.66 | 7.65 | 8.47 | 10.39 | 21.30 | 8.42 | 10.61 | 6.39 | 6.38 |
| MnO | 0.30 | 0.20 | 0.16 | 0.23 | 0.00 | 0.19 | 0.29 | 0.23 | 0.33 | 0.27 | 0.30 | 0.29 | 0.38 | 0.49 | 0.50 | 0.55 | 0.19 | 0.22 | 0.34 | 0.49 | 0.20 | 0.24 | 0.19 | 0.16 |
| MgO | 14.78 | 12.21 | 18.26 | 17.37 | 16.93 | 13.00 | 11.71 | 11.96 | 13.28 | 23.61 | 17.16 | 15.16 | 14.86 | 13.09 | 15.25 | 18.60 | 17.73 | 16.56 | 15.19 | 16.19 | 13.07 | 13.24 | 18.23 | 17.08 |
| CaO | 18.57 | 19.40 | 19.86 | 19.79 | 19.12 | 20.52 | 21.38 | 20.80 | 16.51 | 11.60 | 18.89 | 19.62 | 18.81 | 16.08 | 12.41 | 7.37 | 17.61 | 18.60 | 17.85 | 8.85 | 21.05 | 19.15 | 17.66 | 18.72 |
| Na ₂ O | 0.31 | 0.43 | 0.27 | 0.24 | 0.25 | 0.41 | 0.55 | 0.53 | 0.33 | 0.04 | 0.23 | 0.39 | 0.34 | 0.47 | 0.27 | 0.15 | 0.29 | 0.29 | 0.32 | 0.15 | 0.36 | 0.34 | 0.24 | 0.35 |
| K ₂ O | 0.00 | 0.04 | 0.00 | 0.02 | 0.00 | 0.05 | 0.00 | 0.00 | 0.00 | 0.00 | 0.00 | 0.00 | 0.00 | 0.00 | 0.00 | 0.00 | 0.00 | 0.01 | 0.04 | 0.01 | 0.00 | 0.03 | 0.02 | 0.00 |
| Total | 99.88 | 98.73 | 99.16 | 99.11 | 98.75 | 99.73 | 99.45 | 99.01 | 99.34 | 100.00 | 99.76 | 100.11 | 99.37 | 99.60 | 99.37 | 99.84 | 99.88 | 99.47 | 99.12 | 100.30 | 99.30 | 99.28 | 99.22 | 99.15 |
| Wo | 40.6 | 42.7 | 40.7 | 41.2 | 40.4 | 44.3 | 47.3 | 46.0 | 35.1 | 23.0 | 39.6 | 41.2 | 39.1 | 34.2 | 26.1 | 15.0 | 36.4 | 38.4 | 37.7 | 18.3 | 45.8 | 41.6 | 36.7 | 39.3 |
| En | 44.9 | 37.4 | 52.1 | 50.3 | 49.7 | 39.0 | 36.1 | 36.8 | 39.3 | 65.0 | 50.1 | 44.3 | 43.0 | 38.8 | 44.6 | 52.8 | 51.0 | 47.6 | 44.6 | 46.5 | 39.5 | 40.0 | 52.7 | 49.9 |
| Fs | 14.5 | 19.9 | 7.2 | 8.5 | 9.9 | 16.7 | 16.6 | 17.2 | 25.6 | 12.0 | 10.3 | 14.5 | 17.9 | 27.0 | 29.3 | 32.2 | 12.6 | 14.0 | 17.7 | 35.2 | 14.7 | 18.4 | 10.6 | 10.8 |

Note: Cores of phenocrysts: Analysis nos. 8, 9; rim of phenocryst: 10 (corresponding to Core 9); microphenocrysts: 11, 13, 22, 28; groundmass crystals: 6, 7, 12, 14, 15, 18, 19, 20, 21, 23, 24, 25, 26, 27, 29. Total iron expressed as FeO. Ternary components are computed from structural formulas—Wo = Ca, En = Mg, and Fs = Fe + Mn, normalized to 100%.

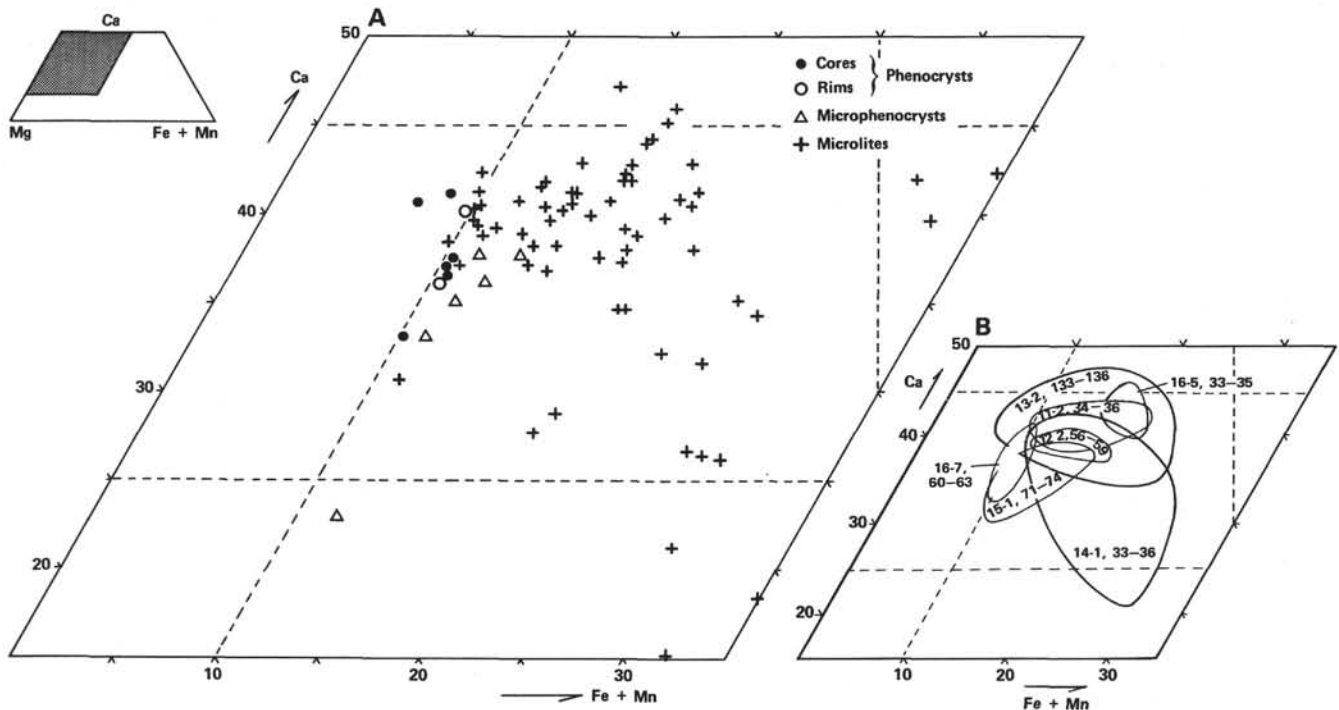


Figure 3. A. Hole 543A clinopyroxene compositions plotted on the Ca-Mg-(Fe + Mn) diagram. B. The patterns of groundmass pyroxene compositions in individual samples (core-section, interval in cm) are indicated. The extreme ferroaugitic compositions have not been considered.

(loss on ignition lower than 1.5 wt.%; K₂O amounts usually less than 0.3%; well-preserved primary plagioclases and clinopyroxenes) closely similar to those presently being emplaced at the Ridge axis.

The trace element compositions also show that these basalts correspond to typically depleted mid-ocean tholeiites: the fresh samples are characterized by very low alkali element contents, a depleted extended Coryell-Masuda plot, and a La/Ta ratio equal to 18. Altered samples show typical trends of alkali metals already observed for oceanic tholeiites.

Comments on Models of Island-Arc Magma Genesis

Leg 78A has provided the finest set of ocean-floor basaltic samples yet obtained, which can be considered, from geophysical and structural points of view, as comparable to basalts subducting beneath an island arc with abundant active magmatism, predominantly of a calc-

alkaline type. In most models of island-arc magma genesis, great importance is given to the dehydration, metamorphism, or even melting of altered oceanic crust, which is supposed to contain 2 to 5 wt. % H₂O when subducted (e.g., Anderson et al., 1980; Gill, 1981). The evidence now obtained from recent drilling of the upper part of the ocean crust in the immediate vicinity of subduction zones (DSDP Legs 66 and 67, Central America; and Leg 78A) shows that in these three cases the basalts themselves are relatively fresh: the values of their loss on ignition are in most cases consistently less than 1.5% (Site 487, Leg 66: Joron et al., 1982; Site 495, Leg 67: Maury et al., 1982). This fact does not mean that water is present only at such low levels; it may well be present at a level up to 5% or more in the subducting ocean crust. The alteration of ocean crust takes place in the first few ten million years after its creation, before the crust is isolated from seawater by a sediment blanket;

Table 4. Feldspars and secondary mineral analyses (wt. %).

| Sample (interval in cm) | 543A-10-3, 27-31 | | | | | | | | 543A-13-2, 133-136 | | | | | | |
|--------------------------------|---------------------|--------|-------|-------|--------|-------|--------|-------|-----------------------|-------|-------|--------|--------|--------|--|
| | 30 | 31 | 32 | 33 | 34 | 35 | 36 | 37 | 38 | 39 | 40 | 41 | 42 | 43 | |
| SiO ₂ | 63.66 | 63.54 | 46.67 | 53.52 | 50.66 | 51.24 | 49.42 | 54.74 | 46.93 | 54.07 | 53.90 | 52.31 | 29.26 | 49.70 | |
| TiO ₂ | 0.00 | 0.00 | 0.00 | 0.03 | 0.12 | 0.08 | 0.09 | 0.18 | 0.02 | 0.02 | 0.07 | 0.09 | 0.11 | 0.01 | |
| Al ₂ O ₃ | 18.10 | 18.42 | 33.47 | 28.50 | 31.18 | 30.24 | 31.98 | 27.55 | 33.55 | 27.69 | 28.07 | 29.31 | 4.40 | 2.40 | |
| Cr ₂ O ₃ | 0.04 | 0.00 | 0.00 | 0.00 | 0.00 | 0.00 | 0.00 | 0.08 | 0.00 | 0.00 | 0.00 | 0.08 | 0.00 | 0.02 | |
| Fe ₂ O ₃ | 0.00 | 0.00 | 0.27 | 0.64 | 0.36 | 0.59 | 0.46 | 0.96 | 0.66 | 1.12 | 0.88 | 1.02 | 40.04* | 25.71* | |
| MnO | 0.00 | 0.00 | 0.00 | 0.04 | 0.07 | 0.05 | 0.00 | 0.00 | 0.07 | 0.01 | 0.00 | 0.00 | 0.01 | 0.00 | |
| MgO | 0.00 | 0.00 | 0.14 | 0.31 | 0.18 | 0.18 | 0.19 | 0.28 | 0.15 | 0.50 | 0.38 | 0.36 | 11.36 | 4.21 | |
| CaO | 0.06 | 0.00 | 17.44 | 12.58 | 14.16 | 13.61 | 15.31 | 11.49 | 16.65 | 11.92 | 11.76 | 13.13 | 1.63 | 0.57 | |
| Na ₂ O | 0.22 | 0.28 | 1.48 | 4.00 | 3.27 | 3.44 | 2.60 | 4.66 | 1.84 | 4.04 | 4.43 | 3.76 | 0.24 | 0.15 | |
| K ₂ O | 18.64 | 18.06 | 0.03 | 0.06 | 0.00 | 0.03 | 0.02 | 0.08 | 0.02 | 0.00 | 0.01 | 0.05 | 0.43 | 8.85 | |
| Total | 100.72 | 100.30 | 99.50 | 99.68 | 100.00 | 99.46 | 100.15 | 99.94 | 99.89 | 99.37 | 99.50 | 100.11 | 87.48 | 91.62 | |
| Or | 97.9 | 97.7 | 0.2 | 0.4 | 0.0 | 0.2 | 0.1 | 0.5 | 0.1 | 0.0 | 0.1 | 0.3 | | | |
| Ab | 1.8 | 2.3 | 13.3 | 36.4 | 29.4 | 31.3 | 23.5 | 42.1 | 16.7 | 38.0 | 40.5 | 34.0 | | | |
| An | 0.3 | 0.0 | 86.5 | 63.2 | 70.6 | 68.5 | 76.4 | 57.4 | 83.2 | 62.0 | 59.4 | 65.7 | | | |

Note: Analyses nos. 30, 31: secondary orthoclase replacing plagioclase phenocrysts; 32, 41: plagioclases; 32-33, 34-35, 36-37, and 38-39 are the cores and rims of phenocrysts respectively 2.7 mm, 1.3 mm, 0.2 mm, and 0.08 mm wide; 40, 41: groundmass plagioclases; 42: chlorite; 43: celadonite. Total iron expressed as Fe₂O₃ for feldspars, FeO (indicated by *) for chlorite and celadonite. Ternary components are computed from structural formulas—Or = K, Ab = Na, An = Ca, normalized to 100%.

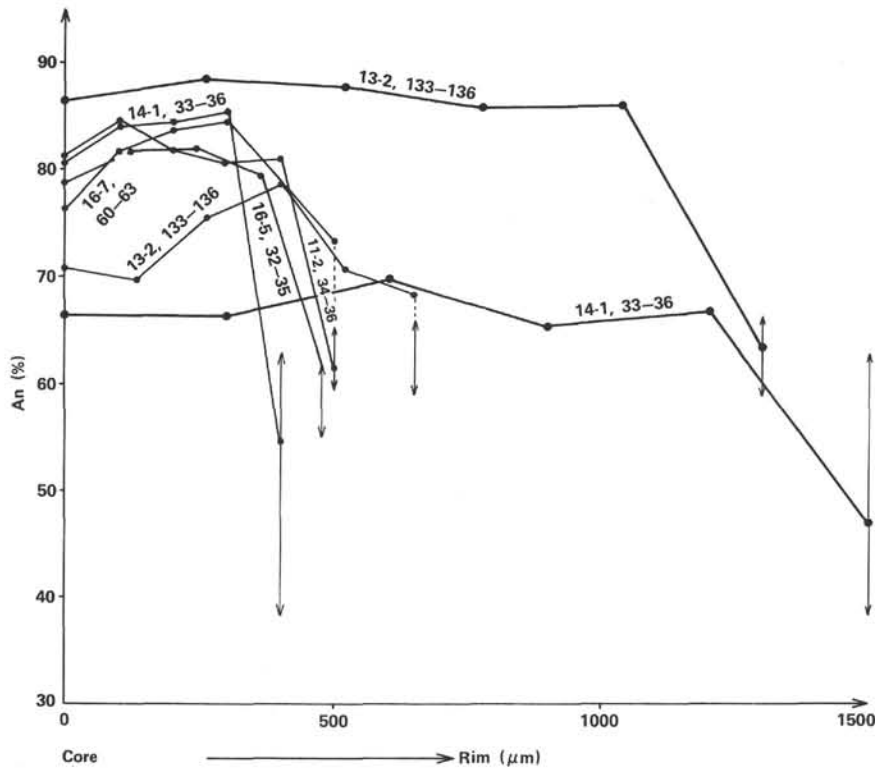


Figure 4. Some patterns of plagioclase zonings in Hole 543A samples. (The vertical double arrows indicate the compositional variations of groundmass plagioclases in the host basalts. Samples are denoted by core-section, interval in cm.)

after this isolation, water remains present in voids between pillows and in fissures, and such water will be more important volumetrically in subduction-zone dehydration processes than that water in the basalts.

ACKNOWLEDGMENTS

We are grateful to the scientific party of Leg 78A for making available to us basalt samples that were recovered from the substratum approaching a subduction zone. J. H. Hawkins and S. H. Bloomer kindly reviewed the manuscript.

REFERENCES

Anderson, R. N., Hasegawa, A., Umino, N., and Takagi, A., 1980 Phase changes and the frequency-magnitude distribution in the upper place of the deep seismic zone beneath Tohoku, Japan. *J. Geophys. Res.*, 85:1389-1398.

Bougault, H., 1980. Contribution des éléments de transition à la compréhension de la genèse des basaltes océaniques. Analyse des éléments traces dans les roches par spectrométrie de fluorescence X [Ph.D. dissert.]. Université de Paris VI, Paris.

Bougault, H., Cambon, P., and Toalhouat, H., 1977 X-Ray spectrometric analysis of trace elements in rocks. Correction for instrumental interferences. *X-Ray Spectrometry*, 6(2):66-72.

- Bougault, H., Joron, J. L., and Treuil, M., 1979. Alteration, fractional crystallization, partial melting, mantle properties from trace element in basalts recovered in the North Atlantic. In Talwani, M., Harrison, C. G. A., and Hayes, D. E. (Eds.), *Deep Drilling Results in the Atlantic Ocean: Ocean Crust*. Am. Geophys. Union., Maurice Ewing Series, 2:352-368.
- Donnelly, T. W., Thompson, G., and Robinson, P., 1979. Very low temperature alteration of the oceanic crust and the problem of the fluxes of potassium and magnesium. In Talwani, M., Harrison, C. G. A., and Hayes, D. E. (Eds.), *Deep Drilling Results in the Atlantic Ocean: Ocean Crust*. Am. Geophys. Union, Maurice Ewing Series, 2:369-382.
- Gill, J. B., 1981. *Orogenic Andesites and Plate Tectonics*: Berlin (Springer Verlag), pp. 230-232.
- Hawkins, J. W., Jr., 1977. Petrologic and geochemical characteristics of margin basin basalts. In Talwani, M., and Pitman, W. C., III (Eds.), *Island Arcs, Deep-Sea Trenches and Back-Arc Basins*: Washington (Am. Geophys. Union) Maurice Ewing Series, 1: 355-366.
- Joron, J. L., Bougault, H., Maury, R. C., and Stephan, J. F., 1982. Basalt from the Cocos Plate, Site 487, Leg 66: petrology and geochemistry. In Watkins, J. S., Moore, J. C., et al., *Init. Repts. DSDP, 66*: Washington (U.S. Govt. Printing Office), 731-734.
- Maury, R. C., Bougault, H., Joron, J. L., Girard, D., Treuil, M., Azéma, J., and Aubouin, J., 1982. Volcanic rocks from Leg 67 sites: mineralogy and geochemistry. In Aubouin, J., von Huene, R., et al., *Init. Repts. DSDP, 67*: Washington (U.S. Govt. Printing Office), 557-576.
- Natland, J. H., 1979. Crystal morphologies in basalts from DSDP Site 395, 23°N, 46°W, Mid-Atlantic Ridge. In Melson, W. G., Rabinowitz, P. D., et al., *Init. Repts. DSDP, 45*: Washington (U.S. Govt. Printing Office), 423-446.
- Nielsen, R. L., and Drake, M. J., 1979. Pyroxene-melt equilibria. *Geochim. Cosmochim. Acta*, 43:1259-1272.
- Sigurdsson, H., and Schilling, S. G., 1976. Spinel in Mid-Atlantic Ridge basalts, chemistry and occurrence. *Earth Planet Sci. Lett.*, 29:7-20.
- Smith, D., and Lindsley, D. H., 1971. Stable and metastable augite crystallization trends in a single basalt flow. *Am. Mineral.*, 56: 225-233.
- Treuil, M., Jaffrezic, H., Deschamp, N., Derre, C., Guichard, F., Joron, J. L., Pelletier, B., Novotry, S., and Courtois, C., 1973. Analyse des lanthanides du Hafnium, du scandium, du chrome, du manganèse, du cobalt, du cuivre et du zinc dans les minéraux et les roches par activation neutronique. *J. Radioanalyt. Chem.*, 18: 55-68.

Wood, D. A., Varet, J., Bougault, H., Corre, O., Joron, J. L., Treuil, M., Bizouard, H., Norry, M. J., Hawkesworth, C. J., and Roddick, J. C., 1979. The petrology, geochemistry, and mineralogy North-Atlantic basalts: a discussion based on IPOD Leg 49. In Luyendyk, B. P., Cann, J. R., et al., *Init. Repts. DSDP, 49*: Washington (U.S. Govt. Printing Office), 597-655.

Date of Initial Receipt: January 10, 1983

Date of Acceptance: August 9, 1983

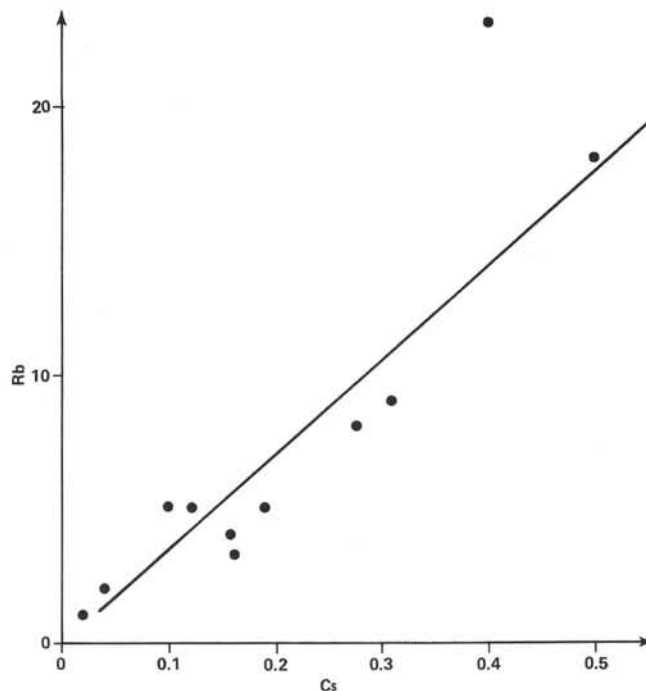


Figure 5. Rubidium (ppm) versus Cs (ppm). (This plot shows the correlation between alkali elements during alteration processes of the oceanic crust. The original values [before alteration] are very low and correspond to the lower values [Rb < 1 ppm, Cs < 0.02 ppm].)

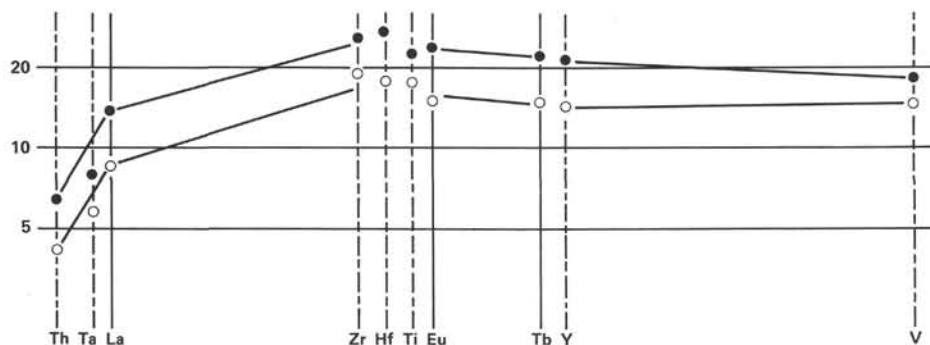


Figure 6. Extended Coryell-Masuda plots. (The concentrations of samples normalized to chondrite concentrations are plotted versus the elements arranged versus their decreasing affinity for the liquid phase of the magma. The two selected samples: ●—543A-12-4, 99-101 cm, the upper one, and ○—543A-16-3, 117-120 cm, the lower one, define the range of variation in Hole 543A. These plots correspond to typical depleted mid-ocean ridge basalts.)

Table 5. Trace element data (ppm), Hole 543A.

| Sample (interval in cm) | Sc | Ti | V | Cr | Mn | Fe | Co | | Ni | | Zn | Rb | Sr | Y | Sr | Nb | Sb | Cs | Ba | La | Eu | Tb | Hf | Ta | Th | U |
|----------------------------|------|-------|-----|-----|------|-------|-----|----|-----|-----|-----|-----|-----|-----|-----|-----|------|------|------|-----|------|------|------|------|------|------|
| | NA | XRF | XRF | XRF | XRF | XRF | XRF | NA | XRF | NA | XRF | XRF | XRF | XRF | XRF | XRF | NA | NA | NA | NA | NA | NA | NA | NA | NA | NA |
| 543A-10-3, 27-31 | 38.7 | 10440 | 357 | 284 | 2960 | 76650 | 37 | 39 | 67 | 69 | 90 | 23 | 130 | 37 | 112 | 6 | 0.23 | 0.40 | 35.0 | 3.5 | 1.39 | 0.83 | 3.05 | 0.22 | 0.15 | 0.07 |
| 543A-11-2, 34-36 | 37.8 | 10200 | 338 | 259 | 2680 | 74970 | 36 | 41 | 78 | 86 | 88 | 9 | 141 | 38 | 116 | 4 | 0.04 | 0.31 | 6.8 | 3.6 | 1.38 | 0.87 | 3.11 | 0.22 | 0.15 | 0.06 |
| 543A-12-2, 56-59 | 41.8 | 11880 | 391 | 258 | 3100 | 81340 | 35 | 38 | 65 | 70 | 92 | 18 | 135 | 46 | 134 | 5 | 0.05 | 0.50 | 10.3 | 4.8 | 1.66 | 1.01 | 3.63 | 0.25 | 0.18 | 0.07 |
| 543A-12-4, 99-101 | 38.6 | 9600 | 343 | 284 | 2400 | 70420 | 41 | 46 | 84 | 91 | 81 | 8 | 132 | 36 | 107 | 4 | 0.04 | 0.27 | 8.1 | 3.7 | 1.42 | 0.82 | 2.92 | 0.20 | 0.15 | 0.05 |
| 543A-13-2, 133-136 | 36.9 | 9300 | 327 | 268 | 2540 | 70050 | 41 | 41 | 95 | 96 | 93 | 5 | 128 | 36 | 111 | 5 | 0.01 | 0.10 | — | 3.2 | 1.31 | 0.75 | 2.65 | 0.18 | 0.13 | 0.06 |
| 543A-13-5, 84-87 | 37.2 | 9300 | 328 | 258 | 2540 | 68950 | 40 | 44 | 90 | 100 | 80 | 5 | 130 | 35 | 107 | 5 | 0.03 | 0.19 | 2.8 | 3.5 | 1.35 | 0.78 | 2.70 | 0.19 | 0.14 | 0.04 |
| 543A-14-1, 33-36 | 37.5 | 8940 | 312 | 254 | 2680 | 68880 | 41 | 45 | 115 | 129 | 75 | 1 | 129 | 35 | 95 | 4 | 0.02 | — | 4.6 | 3.2 | 1.26 | 0.79 | 2.58 | 0.19 | 0.14 | — |
| 543A-15-3, 71-74 | 37.6 | 9060 | 323 | 233 | 2680 | 69580 | 44 | 48 | 106 | 121 | 74 | 1 | 127 | 35 | 95 | 4 | 0.02 | 0.02 | — | 2.7 | 1.27 | 0.75 | 2.61 | 0.19 | 0.13 | 0.05 |
| 543A-16-2, 34-37 | 37.4 | 9720 | 327 | 258 | 2820 | 73150 | 41 | 42 | 92 | 100 | 78 | 2 | 136 | 38 | 111 | 4 | 0.01 | 0.04 | 4.7 | 3.6 | 1.43 | 0.82 | 2.89 | 0.20 | 0.14 | 0.04 |
| 543A-16-3, 117-120 | 36.8 | 9120 | 337 | 283 | 2260 | 65380 | 49 | 53 | 107 | 115 | 90 | 1 | 131 | 31 | 96 | 4 | 0.06 | 0.26 | — | 2.7 | 1.22 | 0.69 | 2.56 | 0.18 | 0.13 | 0.05 |
| 543A-16-5, 32-35 | 36.8 | 9900 | 327 | 256 | 2540 | 72940 | 39 | 42 | 92 | 96 | 83 | 4 | 142 | 38 | 113 | 4 | 0.01 | 0.16 | 6.3 | 3.7 | 1.40 | 0.83 | 2.93 | 0.20 | 0.15 | 0.06 |
| 543A-16-7, 60-63 | 37.5 | 9000 | 331 | 250 | 2400 | 71120 | 44 | 48 | 86 | 88 | 77 | 5 | 129 | 35 | 96 | 5 | 0.04 | 0.12 | 3.8 | 3.1 | 1.24 | 0.76 | 2.61 | 0.19 | 0.14 | — |

Note: NA indicates neutron activation analyses and XRF, X-ray fluorescence analyses.